Combined proteomic and miRNome analyses of mouse testis exposed to an endocrine disruptors chemicals mixture reveals altered toxicological pathways involved in male infertility.

Running title: Proteomics/miRNAs in testis exposed to EDCs

Julio Buñay [1], Eduardo Larriba [3], Daniel Patiño-Garcia [1], Paulina Urriola-Muñoz [1,2], Ricardo D. Moreno [1, *] and Jesús del Mazo [3, *]

[1] Department of Physiology, Pontificia Universidad Católica de Chile, Santiago, Chile.

[2] Chemistry Institute, Pontificia Universidad Católica de Valparaíso, Valparaíso, Chile.

[3] Department of Cellular and Molecular Biology, Centro de Investigaciones Biológicas C.I.B. (CSIC), Madrid, Spain.

[*] Equal contribution authorship

[*]Correspondence to: Ricardo D. Moreno, Department of Physiology, Faculty of Biological Science, Pontificia Universidad Católica de Chile, Alameda 340. 8331150, Santiago, Chile, e-mail: rmoreno@bio.puc.cl, phone: +562-23542885 and Jesús del Mazo, Department of Cellular and Molecular Biology, CIB (CSIC), Ramiro de Maeztu, 9. 28040, Madrid, Spain, e-mail: jdelmazo@cib.csic.es, phone: +34-918373112#4324.

ABSTRACT

The increase in male idiopathic infertility has been associated with daily exposure to endocrine disruptors chemicals (EDCs). Nevertheless, the mechanisms of action in relation to dysregulating proteins and regulatory microRNAs are unknown.

We combined proteomic and miRNome analyses of mouse testis chronically exposed to low doses of a define mixture of EDCs [phthalates: bis (2-ethylhexyl), dibutyl and benzyl-butyl; 4-nonylphenol and 4-tert-octylphenol], administered in the drinking water from conception until adulthood (post-natal day 60/75) and compared them with no-exposed control mice.

We analysed fertility parameters and global changes in the patterns of mice testis proteome by 2D-electrophoresis/mass spectrometry, along with bioinformatic analyses of dysregulated microRNAs, and their association with published data in human infertile patients.

We detected a decrease in the potential fertility of exposed mice associated with changes in the expression of 18 proteins (10 up-regulated, 8 down-regulated). Functional analysis showed that 89% were involved in cell death. Furthermore, we found a group of 23 microRNAs/isomiRs (down-regulated) correlated with six of the up-regulated target proteins (DIABLO, PGAM1, RTRAF, EIF4E, IVD and CNDP2). Regarding this, PGAM1 up-regulation was validated by Western blot and mainly detected in Sertoli cells. Some of these microRNA/protein dysregulations were reported in human testis with spermatogenic failure.

Overall, a chronic exposure to EDCs mixture in human males could potentially lead to spermatogenic failure through changes in microRNA expression, which could post-transcriptionally dysregulate mRNA targets that encode proteins participating in cell death in

testicular cells. Finally, these microRNA/protein dysregulations need to be validated with other EDCs mixtures and concentrations.

Key words:

endocrine disruptors, PGAM1, miRNAs, isomiRs, proteome, spermatogenic failure, infertility.

INTRODUCTION

Endocrine disruptors chemicals (EDCs) such as phthalates and alkylphenols are environmentally widespread man-made chemicals to which humans and wildlife are chronically exposed from fetal life to adulthood (Bergman *et al.*, 2012). At a toxicological level, the effects on male fertility are a hallmark of the exposure to EDCs. This has been documented by epidemiological studies, which report correlations between idiopathic male infertility (specially deterioration in sperm quality and quantity) and high levels of phthalates such as: di-(2-ethylhexyl) phthalate (DEHP), dibutyl phthalate (DBP) and benzyl butyl phthalate (BBP or BzBP); and alkylphenols such as: nonylphenol (NP) and octylphenol (OP) detected in both urine and semen (Pant *et al.*, 2008; Chen *et al.*, 2013). Furthermore, some reports from human fetal testis and experimental murine models of single exposure to these compounds demonstrate that they can act as trigger factors of death in testicular cells (De Jager *et al.*, 1999; Yoshida *et al.*, 2001; Boekelheide *et al.*, 2009; Lambrot *et al.*, 2009). However, the molecular mechanisms involved have not been fully disclosed.

Changes in the global proteomic profile have been detected in ejaculated spermatozoa of idiopathic infertile patients, and are are mainly associated with the folding and degradation of proteins, cytoskeleton and energy metabolism, (Cao *et al.*, 2018, Jodar *et al.*, 2017; Bracke *et al.*, 2018). In relation to the changes in spermatogenesis, recently a quantitative proteomic analyses in testis of infertile patients revealed that over 520 proteins are dysregulated (Alikhani *et al.*, 2017). Overall this data lead to the conclusion that a complex dysregulation of protein expression occurs in testis of patients with idiopathic infertility. However, the causes that originate it remain unsolved.

Inside the regulatory proteins expression mechanisms, the regulation of mRNA expression mediated by microRNAs (miRNAs) and theirs sequence variants or isomiRs have taken relevance. The miRNAs/isomiRs are small non-coding endogenous RNA, which are evolutionarily well-conserved between species and implicated in the negative post-transcriptional regulatory systems in a sequence-specific manner (Guo *et al.*, 2010; Neilsen *et al.*, 2012). In fact, several dysregulated miRNAs in testes of infertile patients have been reported by multiple studies (Abu-Halima *et al.*, 2014; Munoz *et al.*, 2015; Noveski *et al.*, 2016), allowingthe hypothesis that "an aberrant expression of miRNAs could promote certain alterations in spermatogenesis and... be a cause of infertility in males" (Smorag *et al.*, 2012). Additionally, integrative reports of differentially expressed genes and miRNAs in testis of infertile patients have also emerged, which help in exploring miRNA-mRNA interactions and uncovering the molecular regulatory network and therapeutic targets in male infertility (Zhuang *et al.*, 2015; Li *et al.*, 2016).

Our previous reports showed for first time that exposure to EDCs (phthalates and alkylphenols) mixture alters specific miRNAs/isomiRs involved in the control of hormonal status in mice testis (Buñay *et al.*, 2017). However, the consequent effects on protein networks have not been fully addressed. Therefore, the aim of this work was to evaluate a functional association between dysregulated proteins and miRNAs in mouse testis with impaired fertility due to the chronic exposure to low-doses of mixtures of phthalates and alkylphenols. The results showed that some toxicological proteins/miRNAs pathways involved in cell death were altered in mouse testis exposed to an EDCs mixture and have potential relationship with idiopathic human male infertility.

MATERIAL AND METHODS

Animals and ethical statement

All procedures relating to the care and handling of animals were carried out in accordance with the regulations of the Consejo Superior de Investigaciones Cientificas (CSIC) and the Pontifical Catholic University of Chile (PUC), following the European Commission (EC) guidelines (directive 86/609/EEC), and the guides for the Care and Use of Agricultural Animals in Agricultural Research and Teaching by the National Research Council of Chile, respectively. The General Direction of Environment of CAM in Spain (Ref. PROEX 054/15) and the National Fund of Science and Technology (FONDECYT) (No. 1150532) in Chile reviewed and approved all the experimental protocols in this work. C57BL/6J mice were bred at the CSIC or PUC animal facilities under specific, pathogen-free (SPF), temperature- and

humidity-controlled conditions in 12-hour light/dark cycles with ad libitum access to food and water.

EDCs mixture exposure

To emulate chronic human exposure to an environmental EDCs mixture, we designed a murine model of chronic exposure to a defined mixture of 0.3 mg/Kg-bw/day of each of the following phthalates: bis (2-ethylhexyl) phthalate (DEHP), dibutyl phthalate (DBP), benzyl butyl phthalate (BBP) (Sigma-Aldrich, USA), and 0.05 mg/kg-bw/day of each of the following alkylphenols: 4-nonylphenol (NP), 4-tert-octylphenol (OP) (Sigma-Aldrich, USA). The total concentration of the EDCs mixture was 1 mg/kg-bw/day. Phthalates were diluted in DMSO (dimethyl sulfoxide) (Sigma-Aldrich, USA) and alkylphenols were diluted in ethanol. For the control group, we used a mixture of DMSO and ethanol (vehicles) with equivalent intake of 0.25 g/kg-bw/ day and 0.06 g/kg-bw/day, respectively. In this toxicological approach (Buñay *et al.*, 2017, 2018; Patiño-García *et al.*, 2018), the dose of each EDCs was chosen based on the non-occupational exposure in human, which is estimated to range between 0.3 mg/Kg-bw/day and 143 mg/Kg-bw/day (National Toxicology Program, 2003a, 2003b, 2006; Jonsson, 2006; Ademollo *et al.*, 2008; Hines *et al.*, 2011). We ensured that the chosen doses were at least ~1,000-fold lower than the LOAEL values for reproductive traits effects in experimental male animals while still being environmentally relevant doses (Chapin *et al.*, 1999; Nagao *et al.*, 2001; Rider *et al.*, 2010)

The EDCs mixture or control (vehicles) were dissolved in the drinking water of C57BL/6J mice in independent bottles covered with foil. The final dose was calculated

according to the volume of water ingested by the mice and the (bw) recorded in a pilot study and in agreement with data in the literature referring to these parameters. Water intake was controlled each day. The global water intake was not affected by the exposure to EDCs or control. Then, the EDCs mixture or control was administered with ad libitum access, to pregnant mice randomly selected at post-coital day 0.5 (conception) and throughout gestation and lactation. At weaning, only male offspring were selected and maintained at a maximum of four individuals per cage. The administration of the EDCs mixture or control was continued in these mice until adulthood (endpoint: post-natal day 60 and post-natal day 75 for fertility assays) (Buñay *et al.*, 2017, 2018). We choose this model in order to mimic the human where the problems of idiopathic fertility appear from the beginning of their reproductive life. Thus, taking account that the fecundity of male mice declines with age, we consider that the choice of day 75 of age for male mice allows us to make sure that the male mice have good reproductive performance.

All male litter of one pregnant mouse exposed was considered as a statistical unit (n) and we used a minimum of three distinct male litters per group. Within a single litter, the male offspring exposed to EDCs mixture and/or control were considered biological replicates and used in the different test.

Protein extraction

At the specified endpoints, animals were sacrificed, and testes were removed, decapsulated and mechanically homogenized in radioimmunoprecipitation assay buffer (RIPA), along with a protease inhibitor cocktail with 2 mM AEBSF (4-(2-Aminoethyl) benzenesulfonyl

fluoride hydrochloride), 0.3 µM aprotinin, 130 µM bestatin hydrochloride, 14 µM E-64, 1 mM EDTA and 1 µM leupeptin hemisulfate (Sigma-Aldrich, USA). Proteins were purified by centrifugation at 12000 x g at 4 °C for 10 min and subsequently quantified by the method described by Bradford (Bradford, 1976).

For 2D protein electrophoresis, 150 µg of total protein was isolated from testis of adult mice. Sample pooling of three biological replicates from the control groups and the exposed groups were used, each one contributing equally with 50 µg of total protein. Protein purification is described above. These protein extracts were precipitated using a methanol/chloroform protocol (Wessel and Flügge, 1984). Briefly, cold methanol and chloroform were added to the sample tubes previously incubated at 4 ºC and then centrifuged at 13,000 x g at 4 ºC for 15 min. Protein-interfaces were washed and centrifuged twice with cold methanol whereas protein pellets were dried and resuspended in 2x buffer (7 M urea, 2 M thiourea, 4 % [w/v] CHAPS and 0.0003 % [w/v] bromophenol blue). Protein concentration quantification was made with the RC-DC Protein Assay (Bio-Rad, USA).

2D electrophoresis, image acquisition and identification of the peptide footprint

For 2D electrophoresis, aliquots of 150 µg of protein from both control and exposed groups were diluted in a total volume of 350 µl with 2X buffer containing 18.2 M DTT and 0.5 % of IPG buffer solution of ampholytes (pH 3-10) (Bio-Rad, USA) as final concentrations. The first dimension was run on IPG strips (pH 3-10 NL, 17 cm) (Bio-Rad, USA) in a Protean IEF Cell system (Bio-Rad, USA) at 20 ºC. Active rehydration was performed at 50 V for at least 16 h. The IEF steps program was: 300 V for 45 min, linear ramp; 3500 V for 22 h 45 min, rapid

ramp; 5000 V for 30 min, rapid ramp, and 100 V, rapid ramp, until total voltage time reached 80,000 V·h; maximum current limits: 99 µA/strip. Each gel strip was equilibrated in 5 ml of equilibration buffer (50 mM Tris:HCl pH 8.8, 2 % [w/v] SDS; 6 M urea; 30 % [v/v] glycerol) containing 52 mM DTT for 15 min and then in 5 ml of equilibration buffer containing 130 mM iodoacetamide for 15 min.

The second dimension was run in 1.5 mm-thick, 18 x 20 cm SDS-PAGE gels (12% acrylamide). Gels were cast according to the manufactures protocol (Bio-Rad, USA), prepared the day before, and kept at 4 °C before use. Second dimension gels were run at 5 watts/gel for 30 min and then at 17 watts/gel until the BPB front reached the bottom edge, using a cooled Protean II xi Cell (Bio-Rad, USA) and 10 µl of Precision Plus Protein Unstained Standards solution (Bio-Rad, USA) were used as protein markers. Finally, gels were stained with SYPRO Ruby protein gel stain (Bio-Rad, USA) according to the manufacturer instructions. EXQuest Spot Cutter (Bio-Rad, USA) was used to image the gels at different excitation/emission times and to pick the selected spots, which were then subjected to manual tryptic digestion. For digestion, gel pieces were washed first with 50 mM ammonium bicarbonate (Sigma-Aldrich, USA) and then with acetonitrile (ACN) (Scharlau, Spain). Trypsin (Promega, USA) at final concentration of 12.5 ng/µl in 50 mM ammonium bicarbonate solution was added to the gel pieces for 8 h at 37 °C. Finally, 100% ACN containing 0.5% trifluoroacetic acid (TFA) (Sigma-Aldrich, USA) was added for peptide extraction. Tryptic eluted peptides were dried by speed-vacuum centrifugation and resuspended in 6 µl of 30% ACN- 0.1% TFA. Then 1 µl of each peptide mixture was deposited onto an 800 µm AnchorChip (Bruker-Daltonics, USA) and dried at room temperature, and1 µl of matrix solution (3 mg / ml α-cyano-4-hydroxycinnamic acid)

in 33% ACN 0.1% TFA was then deposited onto the digest and allowed to dry at room temperature.

Mass spectrometry (MS) analysis

Samples were analysed with an Autoflex III TOF/TOF mass spectrometer (Bruker-Daltonics, USA). Typically, 1000 scans for peptide mass fingerprinting (PMF) and 2000 scans for MS/MS were collected. Automated analysis of mass data was performed using FlexAnalysis software (Bruker-Daltonics, USA). Internal calibration of MALDI-TOF mass spectra was performed using two trypsin autolysis ions with m/z 842.510 and m/z 2211.105; as for MALDI-MS/MS, calibrations were performed with a fragment ion spectrum obtained from the proton adducts of a peptide mixture covering the m/z 700–4000 region. The typical error observed in mass accuracy for calibration was usually below 50 ppm. MALDI–MS and MS/MS data were combined through the BioTools 3.0 program (Bruker-Daltonics, USA) to interrogate the NCBI non-redundant protein database SwissProt 2014_03 (542782 sequences; 193019802 residues) using MASCOT software 2.3 (Matrix Science, UK). Relevant search parameters were set as follows: enzyme, trypsin; fixed modifications, carbamidomethyl (C); oxidation (M); 1 missed cleavage allowed; peptide tolerance, 50 ppm; MS/MS tolerance, 0.5 Da.

Peptide mass fingerprinting and fragmentation by MS-MALDI-TOF was carried out in the Proteomics and Genomics Facility (CIB-CSIC), a member of ProteoRed-ISCIII network.

Western Blotting

Samples of 20 µg of protein homogenizing were retrieved from the testes of the control groups and the exposed to EDCs groups (n=3) and separated by electrophoresis on a 12% polyacrylamide gel (sodium dodecyl sulfate–polyacrylamide gel electrophoresis) under denaturing and reducing conditions and then transferred to a nitrocellulose membrane (Thermo Scientific, USA) at 350 mA for 2 hours. Next, membranes were blocked with a solution of 3% (w/v) bovine serum albumin 0.1% (v/v) Tween in Tris-buffered saline, pH 7.4, and incubated overnight with the respective primary antibodies for PGAM1 (0.4 ng/µl) (Abbexa, UK) and ß-ACTIN (0.3 µg/µl) (Sigma-Aldrich, USA) as a loading control. Finally, the second incubation took place with their respective secondary antibodies conjugated with horseradish peroxidase (KPL, Gaithersburg, UK) diluted 1:5,000 in blocking solution for 1 hour at room temperature. Peroxidase activity was detected by enhanced chemiluminescence (Pierce Biotechnology, Rockford, IL).

Immunohistochemistry)

PGAM1 was detected in paraffin-embedded cross-sections of testes (n=3) fixed in Bouin's solution for each group and treated with sodium citrate 0.01 M, pH 6, in heat until it boiled and then kept for 10 minutes to expose the antigens. After, the samples were first treated with 3% H_2O_2 for 10 min. Then, to prevent unspecific binding, a standard protein block system (Ultra V block, Thermo Scientific, USA) was applied for 10 min. Primary antibodies were applied at a concentration of (4 ng/µl); samples were incubated overnight at 4°C in a humidified chamber after being washed three times for 5 min in a Tris–HCl buffer, pH 7.6, with 0.3 M NaCl and 0.1% Tween-20. Biotinylated secondary antibody, streptavidin–

biotinylated–peroxidase complex, amplification reagent (biotinyl tyramide) and peroxidase-conjugated streptavidin were applied step-by-step for 10 min each (Thermo Scientific, USA). Afterwards, slides were washed three times for 5 min in a Tris–HCl buffer, pH 7.6, with 0.3 M NaCl and 0.1% Tween-20. Finally, DAB (3,3-diaminobenzidine tetrahydrochloride) Plus Substrate and DAB Plus Chromogen (Thermo Scientific, USA) were applied for 1 min and washed in distilled water. Samples were stained with hematoxylin and observed under a phase contrast microscope (Optiphot-2, Nikon, Tokyo, Japan) and photographed with a digital camera (CoolPix 4500, Nikon, Tokyo, Japan).

Protein functional analyses, expression of miRNA/isomiRs and identification of miRNA-mRNA-protein targets

Protein ontology analyses were performed firstly at the Mouse Genome Informatics (MGI) and Uniprot databases. Protein-protein interactions were analysed by STRING (https://string-db.org/), then functional analysis of GO domains was performed using a Cytoscape plugging ClueGO (Bindea *et al.*, 2009) by a hypergeometric test with a p-value threshold ≤ 0.05.

Small-RNAseq data of testis exposed to EDCs mixture or control were obtained from NCBI Gene Expression Omnibus (GEO) from our previous work: GSE8469 (Buñay *et al.*, 2017). Small-RNAseq data were processed as described. Briefly, MicroRNA identification and quantification were performed by aligned trimmed reads to the mouse genome (mm10) using Bowtie aligner (Langmead *et al.*, 2009) and then using HTSeq script (Anders *et al.*, 2015) with GFF file from miRBase v21. Further, isomiRage software were used for isomiRs detection and

quantification (Muller *et al.*, 2014). We carried out data normalisation and differential expression analysis using the DeSeq tool of the R/Bioconductor software package (Anders *et al.*, 2013).

Correlations between miRNAs and proteins were found using the miRWalk database, combining the searches of three or more databases, along with the validated mRNA targets reporter in miRWalk and a validated miRNA:mRNA database, DIANA-TARbase v7.0 (Vlachos *et al.*, 2015). The interaction map was performed using a Cytoscape.

Fertility assay

Gestational rate, fertility index and potential fertility were calculated according to Garcia *et al.*, (2012). Representative animals of each "n" per group were selected randomly and treated (control and EDCs mixture) until post-natal day 75 to ensure their potential fertility. After this period, males were placed in individual cages and cohabited with two unexposed adult females for 8 days (to ensure at least two complete female estrous cycles). Vaginal plugs were checked every day early in the morning (08:00 - 09:00 h). All females with vaginal plug were set apart and placed in individual cages. An effective pregnancy was confirmed by the increase of the body weight.

Between the days 18 to 20 post-detection of the vaginal plug, a group of females were sacrificed to quantify the number of implantations and reabsorptions in each uterine horn and the fetal mortality rate (number of reabsorptions / number of implantations x 100). Then, ovaries were extracted, fixed in Bouin solution and processed for histological analysis. Serial sections of each ovary were stained with hematoxylin-eosin, and the number of corpora lutea

per ovary was quantified. Another group of pregnant females was maintained until the delivery. Between the postnatal day 1 or 3, the number of newborns was quantified.

Statistical analysis

For the selection and quantification of spots of interest in 2D gels, PDQuest™ V8.0 (Bio-Rad) was used. First, a reference gel was created from images of the analysed gels. Then, each one of these gels were aligned with the reference gel. Spot quantification in relation to the protein levels was calculated considering the intensities of all pixels within the defined boundary previously normalized. Finally, the quantitative data of each spot were normalised using a nonparametric linear regression analysis (LOESS) to compare each expression level. This approach combined with MS, enabled us to identify the PPIA protein levels with no significant changes between the two groups (control and exposed to EDCs). As others studies suggest, PPIA is suitable to be used as an internal control (Kim *et al.*, 2014). Consequently, PPIA was used as an endogenous reference protein (housekeeping) in order to perform a second normalisation/comparison of the proteins identified by MS.

In mass spectrometry analysis, mascot total scores greater than 75 were considered significant ($p<0.05$).

Reproductive outcome in male mice exposed to EDCs mixture was analysed by Chi-square test, umpaired t-test and one-way ANOVA along with Dunnett's post hoc test, using GraphPad Prism version 5.0. (GraphPad Software, USA).

RESULTS

Chronic exposure to a EDCs mixture and fertility in male mice

In previous works, we showed that exposure to a single EDC or mixture of EDCs induces an increase in the body weight, a decrease in testis relative weight, testis lesions and hormonal status changes (Buñay *et al.*, 2017, 2018). In the present work, while assessing the fertility of males exposed to a specific EDCs mixture, we found that there were no significant differences in several reproductive parameters such as: gestational rate, fertility index and potential fertility, when compared to control groups (Supplementary Table I). Interestingly, in the exposed groups, not all males seem to be equally affected by the treatment. We identified four males from different litters which, once analysed by ANOVA, presented a decrease in potential fertility. Furthermore, when mating resulted in pregnancy, the number of reabsorptions and the rates of pre-implantation loss and fetal mortality were increased (Figure 1 and Supplementary Table I).

Changes in the proteome profile of mouse testis exposed to EDCs mixture

First, to detect changes of testicular proteins levels in mice exposed to EDCs, we performed a global approach and evaluated the mouse testis proteome using 2D electrophoresis comparing exposed mice with controls. We analysed a total of 246 spots/proteins matched by PDQuest software and normalised by LOESS. Based on the differential spot intensities observed, only those proteins that change more than 1.2-fold in exposed versus control groups were taken into account. This approach allowed us to select 21 spots of unequal signals, plus one spot (8102) randomly selected among those of equal relative abundance in all gels (Supplementary Figure 1). These 22 spots/proteins were excised from the gels for further

identification of peptide mass fingerprint by MS-MALDI-TOF. Three spots (904, 1302 and 9104) could not be identified mainly due to low signals. But this experimental approach allowed us to correctly identify 19 spots/proteins. Of these identified proteins, 10 were classified as up-regulated and 8 as down-regulated in testis exposed to EDCs mixture (Figure 2A-B, Table 1); the spot/protein named as 8102 was identified as Peptidyl-prolyl cis-trans isomerase A (PPIA) and no significant changes were detected (Figure 2C, Table 1). It is worthy to note that in our previous work, with the same exposure model, we did not detect changes in the levels of *Ppia* mRNA (Buñay et al., 2017), and therefore used this transcript as an endogenous reference gene (Radonić *et al.*, 2004). A second normalisation using PPIA found that the upregulated/downregulated proteins previously identified in the EDCs group had a minimum of 1.2-fold change (Supplementary Figure 2). Then we decided to validate our 2D electrophoresis/MS results by using western blot and immunohistochemistry. To this end we chose PGAM-1 as it was identified among those proteins up-regulated by 2D electrophoresis/MS. Through Western blot, we found a significant increase in the protein levels of PGAM1 in testes of mice exposed to EDCs mixture. This result was similar to the one observed with 2D electrophoresis/MS. In addition, by immunohistochemistry, PGAM1 localised preferably in Sertoli and interstitial cells both in control and EDCs treated mouse testes. No obvious change in localisation was detected between these populations (Figure 3B).

A bioinformatic analysis of dysregulated proteins detected by 2D electrophoresis/MS was performed, disclosing some protein-protein interaction networks (Supplementary Figure 3). Gene ontology annotation of differentially expressed proteins showed an enrichment in the process of cellular response to stress, in metabolic processes and in protein folding pathways

(Figure 4A). Furthermore, we found that eight up-regulated proteins (DIABLO, HINT1, EIF4E, PSMB4, CNDP2, NME2, PGAM1 and IVD) and all down-regulated proteins (VDAC2, PGP, HSPA8, FKBP4, PDIA3, GSTM2, GSTM7 and CCT2), which represent 89% of all dysregulated proteins (16 out of 18) were involved in different steps of cell death (Figure 4B). As for the other two up-regulated proteins, MP1 is involved in metabolic processes and RTRAF in the regulation of transcription as an RNA binding protein (Table I). Therefore, cell death seems to be the major dysregulated pathway at the protein level.

Association between proteins and miRNAs differentially expressed in mouse testis exposed to EDCs mixture

Integrative in-silico analyses revealed that 23 miRNAs/isomiRs (differentially down-regulated in our previous studies; Buñay *et al.*, 2017) may be associated with six up-regulated proteins (33.3% of total dysregulated proteins), considering the post-transcriptional regulatory roles of identified miRNAs/isomiRs over the corresponding target transcripts encoding identified proteins (Figure 5A). The analyses did not show correlation between down-regulated proteins and up-regulated miRNAs. An integrative map showed that transcripts for DIABLO, PGAM1, RTRAF, EIF4E, IVD and CNDP2 were targets of more than one down-regulated miRNA/isomiRs, which suggested higher potential efficiency in their expected post-transcriptional regulation (Figure 5B and Supplementary Table II). For example, the over-expression of DIABLO and EIF4E could be induced as consequence of down-regulation of five and eight miRNAs/isomiRs, respectively (Figure 5B). In addition, we have identified two isomiRs (*miR-30c-5p_trim2* and *miR-497a-5p_UA_3prime*) whose canonical miRNAs are

reported in the DIANA-TARbase v7.0 as validated for specific transcripts: *miR-30c-5p*: *Diablo* and *miR-497a-5p*: *Ivd* mRNAs. As the detected isomiRs have only different 3' ends (the corresponding 5' seed regions sequence of these isomiRs are the same that the canonical miRNAs). Consequently, it can be expected that the target should be the same for each dysregulated miRNA/isomiR. Furthermore, we showed that the 3' UTR of *Eif4e* mRNA can be targeted by both the *miR-15b-5p* (canonical miRNA) and its isomiR *miR-15b-5p_AA_3prime*, and this interaction is conserved in humans (Figure 5C). This finding might explain the correlation between six identified proteins and the loss of miRNAs/isomiRs with targets in the corresponding mRNAs encoding such proteins, as was detected in testis from mice exposed to the EDCs mixture.

Changes in the expression of proteins and miRNAs in mouse testis exposed to EDCs mixture are linked with idiopathic male infertility

Since some animals exposed to the EDCs mixture showed a decrease fertility, we hypothesised that some of the deregulated protein and miRNA/isomiRs could be also dysregulated in human testis of infertile man.

To assess this comparative analysis, we selected a recent study of label-free quantitative shotgun proteomics on testicular tissue from patients with non-obstructive azoospermia, including maturation arrest (MA) and Sertoli cell only syndrome (SCOS) (Alikhani *et al.*, 2017). The results revealed eight common dysregulated proteins (Figure 6A) in testes from azoospermic men and those of mice exposed to the EDCs mixture. These eight common

proteins represented 44% of proteins dysregulated by EDCs in mice, all of them involved in cell death (EIF4E, PGAM1, DIABLO, PSMB4, PDIA3, CCT, HSPA and GST).

Then, we selected from the literature three similar reports of significant changes in the expression of miRNAs (at least 2-fold changes) in testicular biopsies of patients with MA and SCOS syndromes (Abu-Halima *et al.*, 2014; Munoz *et al.*, 2015; Noveski *et al.*, 2016). These data were contrasted with the list of miRNAs that were differentially expressed by the exposure to EDCs mixture, as previously detected (Buñay *et al.*, 2017). We found two miRNAs (*miRNA-15b* and *miRNA-34b*) that were reported dysregulated in every work on human testis with spermatogenic failure and in our previous work in mice exposed to EDCs. Moreover, three miRNAs were coincidently found only in patients with MA and SCOS reported by Abu Halima et al., 2014 (Abu-Halima *et al.*, 2014) and mice exposed to EDCs mixture *(miR-382, miR-18a, and miR-378)* (Figure 6B). These observations suggested that proteins and miRNAs differently expressed by the exposure to EDCs mixture might be related to spermatogenic failure and associated with the risk of exposure to EDCs of human populations.

DISCUSSION

This work shows a global integrative profile of dysregulated proteins/miRNAs in testes of mice exposed to a mixture of phthalates and alkylphenols, suggesting that chronic exposure to an EDCs mixture during their development might be a plausible cause for idiopathic male infertility.

Male mice are sexually mature when they are around 42 to 49 days old. At this age, each spermatogenesis cycle takes about 35 days to be completed (Griswold, 2016). Although

414 protein/miRNAs expression analyses and fertility tests were performed in 60- and 75-days old
415 animals respectively, we believe that this 15-day difference should not affect the correlation of
416 results since both are in the adult fertile period.

417 As a whole, mice exposed to EDC mixtures did not present significant changes in
418 global fertility. According to this preliminary study, we can not be certain that subfertility is
419 more likely present in the exposed group than in the control group. However, the potential
420 fertility based on the increase of the number of preimplantation losses and reabsorptions was
421 significantly compromised within a sub-group of exposed animals which could be due to: 1)
422 differences in the relative individual susceptibility at the exposure level, from early periods of
423 gonadal development, 2) maternal physiology, 3) differences in the amount of milk intake
424 during lactation and 4) differences in metabolic rate, accumulation, elimination and/or global
425 detoxification rates of EDCs between animals. These observations might mirror the
426 discrepancy in epidemiological data reports in human adult males, pregnant women and
427 children and the association of adverse effects due to the single and mixed exposure to EDCs
428 (Hou *et al.*, 2015; Birks *et al.*, 2016; Sifakis *et al.*, 2017). Therefore, future fertility trials should
429 be performed in greater number of mice covering longer exposure times and different aging to
430 validate the tendency shown in this work. Furthermore, we indicate that new specific
431 epidemiological studies are necessary in the human population with different grades of
432 exposure to EDCs in order to evaluate the impact on male reproductive health.

433 By 2D/MS proteomic analysis, we detected deregulation of 18 proteins in the testes of
434 mice exposed to the EDCs mixture. In this proteomic approach, we used a sample pooling,
435 which is a validated and commonly used option (Weinkauf *et al.*, 2006; Diz *et al.*, 2009; Karp

436 and Lilley, 2009). However, it is important to state that this proteomic study should be seen as a
437 biological averaging (Karp and Lilley, 2009) and that the expression of several proteins
438 observed as dysregulated must be validated through different approaches in future studies.

439 Our previous reports and other studies have indicated that exposures to EDCs
440 mixtures induce apoptosis of germ cells which is also well correlated with the decrease in
441 fertility reported in this work (Manikkam *et al.*, 2013; Buñay *et al.*, 2017, 2018). We found,
442 through developmental analysis, that some forms of GST, for example GSTM2, are down-
443 regulated in normal adults compared to prepuberal mice (Paz *et al.*, 2006), which was in
444 agreement with the higher expression of this GST isoform in Sertoli and spermatogonia cells
445 than in spermatocytes and spermatids (Yu *et al.*, 2003). The decrease in the expression of two
446 glutathione S-transferases (GSTM2 and GSTM7) detected in our 2D proteomic analysis,
447 suggests that the EDCs mixture is affecting the testis during development since the early
448 differentiation stages. In fact, the depletion of antioxidant enzymes is a known mechanism of
449 oxidative stress and cell death. Thus, the decrease in these GSTs levels in testis after exposure
450 to the EDCs mixture would be in opposition to its cytoprotective role and directly involved in
451 mechanism of oxidative stress to induce sperm DNA damage and male infertility.

452 New in-vitro evidence show that endoplasmic reticulum (ER) stress is an early driver
453 of the EDC-mediated perturbations (Rajamani *et al.*, 2017). In this way, our in-vivo approach
454 in mouse testis exposed to the EDCs mixture identified a group of dysregulated proteins
455 involved in ER stress. Firstly, the over-expression of the proteasome subunit beta type-4
456 (PSMB4) responsible of proteasome assembly and protein degradation (Hirano *et al.*, 2008)
457 was correlated with the decrease in at least three proteins expression. One of them, PDIA3 is a

chaperone located at the ER that modulates the thiol-disulphide status of proteins and is considered a survival factor. In-vitro assays found that some EDCs affect the PDIA activity (Klett *et al.*, 2010), and further evidence shows that PDIA3 has the capacity of binding with 17β-estradiol (Primm and Gilbert, 2001, Wong *et al.*, 2017), a hormone that was previously reported as decreased in mouse testis exposed to EDCs mixture (Buñay *et al.*, 2017). Another down-regulated protein was the cytosolic chaperone CCT2, a protein particularly involved in the folding of cytoskeletal and cell cycle proteins (actin, tubulin and cyclin-E), which is related with PSMB4 (up-regulated). Consequently, altered folding of these proteins may stop the cell cycle, cause an ER stress response, disrupt the mitochondria and induce apoptosis in somatic or germ cells. In addition, CCT2 increases its expression from prepuberal to adult mice, suggesting an association with late spermatogenesis (Paz *et al.*, 2006). Finally, the down-regulation of heat-shock cognate protein HSPA8 was also present. HSPA8 participates in the response to ER stress with the pivotal role of correcting the folding of nascent polypeptides and then cooperates in the re-folding of misfolded proteins. At the same time PSMB4, PDIA3, CCT and HSP are found dysregulated in testicular biopsies from patients with SCOS and MA (Alikhani *et al.*, 2017). Therefore, the interplay of these proteins of ER stress could be implicated in germ-cell death induced by EDCs.

Many efforts have been made to identify miRNAs involved in spermatogenic failure (Abu-Halima *et al.*, 2014; Munoz *et al.*, 2015; Noveski *et al.*, 2016). Currently, new approaches with small non-coding RNA sequencing (sncRNA-Seq) suggest that changes of miRNA variants or isomiRs (more than canonical miRNAs) could better describe a pathological state (Guo *et al.*, 2011; Kozlowska *et al.*, 2013; Telonis *et al.*, 2015). In this sense, at the

480 reproductive level, the changes in isomiRs expression due to the EDCs exposure could have a
481 more relevant role than canonical miRNAs. Thus, we suggest that future studies focused on
482 changes in the miRNome of infertile subjects (male and female) should include analyses of
483 isomiRs.

484 DIABLO (SMAC) is a relevant pro-apoptotic protein with ubiquitous expression in
485 testicular cells that showed, by 2D electrophoresis/MS, an increased expression in the testes of
486 mice exposed to EDCs mixture. Interestingly, preliminary reports by immunohistochemistry
487 have not showed differences in the expression of DIABLO in azoospermic patients compared
488 to subjects with normal testicular histology (Bozec *et al.*, 2008). However, Jaiswal and
489 collaborators (Jaiswal *et al.*, 2015) demonstrated that protein expression of DIABLO increased
490 in infertile human testes with hypospermatogenesis, MA and SCOS. And recently, the study of
491 global proteome profile in human testis affected by MA or SCOS have corroborated that
492 DIABLO expression is dysregulated (Alikhani *et al.*, 2017). Thus, the increase in DIABLO is
493 directly related with the disorder of regulation of apoptosis in its pathogenesis (Takagi *et al.*,
494 2001). In addition, it has been detected that a lack of gonadotropins and androgens causes the
495 increase of DIABLO expression and its translocation to the cytoplasm in spermatocytes (Vera
496 *et al.*, 2006). Moreover, exposure to phthalates metabolites with antiandrogenic effect such as
497 MEHP induces (via decrease of PI3K / AKT and increase of NF-Kβ) germ cell apoptosis by
498 increasing the levels of DIABLO (Rogers *et al.*, 2008). Here, we suggest that the increase of
499 DIABLO is linked to the exposure to EDCs mixture in a new mechanism that involves the
500 down-regulation of miRNA/isomiRs.

501 Another up-regulated protein was EIF4E, whose overexpression is associated with

oncogenesis and metastatic progression in humans (Hsieh and Ruggero, 2010; Siddiqui and Sonenberg, 2015). Furthermore, some studies have reported that somatic cell viability, chromosome condensation, cytokinesis during the meiotic division and normal production of functional sperm in spermatogenesis requires EIF4E activity (Amiri *et al.*, 2001; Ghosh and Lasko, 2015). In addition, in a previous study, we found that changes in the expression of EIF4F complex including *Eif4E* depend on the type of EDCs and the time of exposure (López-Casas *et al.*, 2012). The increase of the level of EIF4E could be a consequence of the loss of post-transcriptional control due to a decrease in the level of one canonical miRNA (*miR-15b-5p*) and seven doubly-adenylated 3′ end isomiRs, targeting its 3'-UTR. This miRNA regulation is also preserved in the human *EIF4E* 3'UTR. At the same time, both EIF4E and *miR-15b* are recurrently dysregulated in testicular biopsies of patients with spermatogenic failure, which suggests a novel mechanism whereby the exposure to EDCs might decreases fertility and should be studied in depth in infertile male patients.

Interestingly, the mitochondrial protein Isovaleryl-CoA dehydrogenase (IVD) was found over-expressed and it increases in response to lipid overload, which is correlated with the obesogenic effect and cholesterol increase reported by the exposure to EDCs (Heindel *et al.*, 2015). Our in-silico data show that the *Ivd* transcript is targeted by one canonical miRNA (*miR-15b-5p*) and the isomiRs *miR-15b-5p_AA_3prime* along to three more down-regulated isomiRs. Therefore, an overexpression of IVD due to the loss of the post-transcriptional control by miRNAs/isomiRs might promote high β-oxidation of free fatty acids and catabolism of proteins that are related to stress in the ER and increased mitochondrial ROS (Tumova *et al.*, 2015),

thus generating mitochondrial dysfunctions commonly detected in spermatozoa of infertile patients.

Similarly, an important enzyme in the glycolytic pathway, PGAM1, was found to be up-regulated in mouse testis exposed to EDCs. In addition, by immunohistochemistry we found that PGAM1 was preferentially expressed in Sertoli and interstitial cells. However, in relation to the protein levels, IHQ analysis could not validate the data obtained by WB and 2D/MS, possibly due to differences in the treatments of the samples related to the fixation method or the epitope retrieval (Uhlen *et al.*, 2016). The increase in PGAM1 suggests that the exposure to EDCs modified the glycolytic profile in somatic cells, particularly in Sertoli cells to subsequently alter the energetic metabolic role supplying germ cells and induce germ cell death. In testicular biopsies from infertile men dysregulated levels of PGAM1 were found (Alikhani *et al.*, 2017), specifically down-regulated in severe hypospermatogenesis and overexpressed in SCOS, which is associated with an inhibition of proliferation and apoptosis (Zhang *et al.*, 2015). Here, we presented the first evidence of post-transcriptional control of PGAM1 mediated by isomiRs, suggesting that these interactions could also be used as biomarkers in male infertility.

Another up-regulated protein was the cytosolic nonspecific dipeptidase 2 (CNDP2). However, its function and implication in human fertility is not clear. Apparently, CNDP2 has more than one enzymatic activity and when increased, it activates p38 and JNK/MAPK pathways to induce cell apoptosis (Zhang *et al.*, 2014). Moreover, recent research on the enzymatic activity of CNDP2 in the cellular metabolome has indicated that this protein can degrade lactate to its metabolites N-lactoil-amino acids (N-lac-Phe) (Jansen *et al.*, 2015). In

545 previous work, we indicated that lactate is a survival factor of spermatocytes (Bustamante-
546 Marín *et al.*, 2012). Although the function of lactate metabolites is unknown, it suggests that
547 the degradation of lactate via an increase in the expression and enzymatic activity of CNDP2
548 could be a new mechanism that modulates germ cell apoptosis. Our analyses indicated that the
549 increase in CNDP2 expression would be associated with the loss of the post-transcriptional
550 control mediated by *miR-23a-3p_AA_3prime*, *miR-320-3p_AAA_3prime*, and the joint action of
551 *miR-3085-3p/miR-3085-3p_UA_3prime*. This supports our hypothesis that isomiRs could
552 participate along with the corresponding canonical miRNAs in the regulation of mRNA targets
553 during spermatogenesis, which can be altered by the exposure to EDCs, triggering changes in
554 metabolic and cell stress pathways.

555 Finally, it is important to remark the possible central role of the down-regulation of
556 *miRNA-15b-5p* and their isomiR (*miR-15b-5p_AA_3prime*) in male infertility, which suggests
557 that a decrease of *miRNA-15b-5p* and/or their isomiR could be a novel biomarker to be used to
558 diagnose patients with subfertility potentially induced by the exposure to EDCs. However, this
559 remains to be epidemiologically and experimentally tested.

560 A group of dysregulated proteins that correlate with somatic and/or germ cell death
561 includes the down-regulated VDAC2, PGP, GSTM2, GSTM7 and the up-regulation of HINT1.
562 We did not find any associated miRNAs that could explain the dysregulation of these proteins,
563 except *HINT1* that is a *bone fide* target of *hsa-miR-15b-5p* (DIANA-TarBase v7.0) in human
564 cells lines. Therefore, there must be additional mechanisms and regulatory molecules that work
565 cooperatively and are mediating the adverse effects of EDCs on male fertility. This matter
566 should be addressed in future studies.

In conclusion, this work is the first report of integrative data from proteomics and miRNAs/isomiRs, which aims to clarify the molecular mechanisms that are affecting male fertility due to the exposure to mixture of phthalates and alkylphenols. Also, it is tempting to envision the possibility of establishing miRNAs pathways as a specific and effective pharmacological therapy for certain types of primary testicular failure.

ACKNOWLEDGMENTS:

We would like to thank MSc. Leonor Cruz Fernandes for the English editing.

AUTHORS' ROLES:

J.B., R.D.M. and J.d.M. designed the research; J.B., D.P-G., and P.U-M., performed the experiments; J.B. and E.L. contributed new analytic tools; J.B., E.L., R.D.M. and J.d.M. analysed data; and J.B., E.L, R.D.M. and J.d.M. wrote the paper.

FUNDING:

This work was supported by grants from FONDECYT 1150352 to R.D.M., FONDECYT 3160273 to P.U-M and CONICYT 21120505 to J.B., Chile, and MINECO BFU2013-42164-R and BFU2017-87095-R to J. d. M., Spain.

CONFLICT OF INTEREST:

None declared.

REFERENCES

Abu-Halima M, Backes C, Leidinger P, Keller A, Lubbad AM, Hammadeh M, Meese E. MicroRNA expression profiles in human testicular tissues of infertile men with different histopathologic patterns. *Fertil Steril* 2014;**101**:78-86.

Ademollo N, Ferrara F, Delise M, Fabietti F, Funari E. Nonylphenol and octylphenol in human breast milk. *Environ Int* 2008;**34**:984–987.

Alikhani M, Mirzaei M, Sabbaghian M, Parsamatin P, Karamzadeh R, Adib S, Sodeifi N, Gilani MAS, Zabet-Moghaddam M, Parker L, *et al.* Quantitative proteomic analysis of human testis reveals system-wide molecular and cellular pathways associated with non-obstructive azoospermia. *J Proteomics* 2017;**162**:141–154.

Amiri a, Keiper BD, Kawasaki I, Fan Y, Kohara Y, Rhoads RE, Strome S. An isoform of eIF4E is a component of germ granules and is required for spermatogenesis in C. elegans. *Development* 2001;**128**:3899–3912.

Anders S, McCarthy D, Chen Y, Okoniewski M, Smyth G, Huber W, Robinson M. Count-based differential expression analysis of RNA sequencing data using R and Bioconductor. *Nat Protoc* 2013;**8**:1765–1786.

Anders S, Pyl PT, Huber W. HTSeq-A Python framework to work with high-throughput

611 sequencing data. *Bioinformatics* 2015;**31**:166–169.
612 Bergman Å, Heindel J, Jobling S, Kidd K, Zoeller RT. State of the science of endocrine
613 disrupting chemicals. *Toxicol Lett* 2012;**211**:S3.
614 Bindea G, Mlecnik B, Hackl H, Charoentong P, Tosolini M, Kirilovsky A, Fridman WH, Pagès
615 F, Trajanoski Z, Galon J. ClueGO: A Cytoscape plug-in to decipher functionally grouped
616 gene ontology and pathway annotation networks. *Bioinformatics* 2009;**25**:1091–1093.
617 Birks L, Casas M, Garcia AM, Alexander J, Barros H, Bergström A, Bonde JP, Burdorf A,
618 Costet N, Danileviciute A, *et al.* Occupational exposure to endocrine-disrupting chemicals
619 and birth weight and length of gestation: A european meta-analysis. *Environ Health*
620 *Perspect* 2016;**124**:1785–1793.
621 Boekelheide K, Kleymenova E, Liu K, Swanson C, Gaido KW. Dose-dependent effects on cell
622 proliferation, seminiferous tubules, and male germ cells in the fetal rat testis following
623 exposure to di(n-butyl) phthalate. *Microsc Res Tech* 2009;**72**:629–638.
624 Bozec A, Amara S, Guarmit B, Selva J, Albert M, Rollet J, El Sirkasi M, Vialard F, Bailly M,
625 Benahmed M, *et al.* Status of the executioner step of apoptosis in human with normal
626 spermatogenesis and azoospermia. *Fertil Steril* 2008;**90**:1723–1731.
627 Bracke A, Peeters K, Punjabi U, Hoogewijs D, Dewilde S. A search for molecular mechanisms
628 underlying male idiopathic infertility. *Reprod Biomed Online* 2018;36: 327-339.
629 Bradford M. A rapid and sensitive method for the quantiWcation of microgram quantities of
630 protein utilizing the principle of protein– dye binding. *Anal Biochem* 1976;**72**:248–254.
631 Buñay J, Larriba E, Moreno RD, del Mazo J. Chronic low-dose exposure to a mixture of
632 environmental endocrine disruptors induces microRNAs/isomiRs deregulation in mouse

concomitant with intratesticular estradiol reduction. *Sci Rep* 2017;**7**:3373.

Buñay J, Larriba E, Patiño-Garcia D, Cruz-Fernandes L, Castañeda-Zegarra S, Rodriguez-Fernandez M, del Mazo J, Moreno RD. Differential effects of exposure to single versus a mixture of endocrine-disrupting chemicals on steroidogenesis pathway in mouse testes. *Toxicol Sci* 2018;**161**:76-86.

Bustamante-Marín X, Quiroga C, Lavandero S, Reyes JG, Moreno RD. Apoptosis, necrosis and autophagy are influenced by metabolic energy sources in cultured rat spermatocytes. *Apoptosis* 2012;**17**:539–550.

Chapin RE, Delaney J, Wang Y, Lanning L, Davis B, Collins B, Mintz N, Wolfe G. The effects of 4-nonylphenol in rats: a multigeneration reproduction study. *Toxicol Sci* 1999;**52**:80–91.

Chen M, Tang R, Fu G, Xu B, Zhu P, Qiao S, Chen X, Xu B, Qin Y, Lu C, *et al.* Association of exposure to phenols and idiopathic male infertility. *J Hazard Mater* 2013;**250**–**251**:115–121.

Diz AP, Truebano M, Skibinski DO. The consequences of sample pooling in proteomics: An empirical study. *Electrophoresis* 2009;**30**:2967–2975.

de Jager C, Bornman MS, van der Horst G. The effect of p-nonylphenol, an environmental toxic ant with oestrogenic properties, on fertility potential in adult male rats. *Andrologia* 1999;**31**:99–106.

Garcia PV, Barbieri MF, Perobelli JE, Consonni SR, Mesquita SdeF, Kempinas WdeG, Pereira LA. Morphometric-stereological and functional epididymal alterations and a decrease in fertility in rats treated with finasteride and after a 30-day post-treatment recovery period.

655 *Fertil Steril* 2012;**97**:1444–1451.
656 Ghosh S, Lasko P. Loss-of-function analysis reveals distinct requirements of the translation
657 initiation factors eIF4E, eIF4E-3, eIF4G and eIF4G2 in Drosophila spermatogenesis. *PLoS*
658 *One* 2015;**10**: e0122519.
659 Griswold MD. Spermatogenesis: The Commitment to Meiosis. *Physiol Rev* 2016;**96**:1–17.
660 Guo H, Ingolia NT, Weissman JS, Bartel DP. Mammalian microRNAs predominantly act to
661 decrease target mRNA levels. *Nature* 2010;**466**:835–840.
662 Guo L, Yang Q, Lu J, Li H, Ge Q, Gu W, Bai Y, Lu Z. A comprehensive survey of miRNA
663 repertoire and 3′ addition events in the placentas of patients with pre-eclampsia from high-
664 throughput sequencing. *PLoS One* 2011;**6**: e21072.
665 Heindel JJ, Newbold R, Schug TT. Endocrine disruptors and obesity. *Nat Rev Endocrinol*
666 2015;**11**:653–661.
667 Hines CJ, Hopf NB, Deddens JA, Silva MJ, Calafat AM. Estimated daily intake of phthalates in
668 occupationally exposed groups. *J Expo Sci Environ Epidemiol* 2011;**21**:133–141.
669 Hirano Y, Kaneko T, Okamoto K, Bai M, Yashiroda H, Furuyama K, Kato K, Tanaka K,
670 Murata S. Dissecting beta-ring assembly pathway of the mammalian 20S proteasome.
671 *EMBO J* 2008;**27**:2204–2213.
672 Hou JW, Lin CL, Tsai YA, Chang CH, Liao KW, Yu CJ, Yang W, Lee MJ, Huang PC, Sun
673 CW, *et al.* The effects of phthalate and nonylphenol exposure on body size and secondary
674 sexual characteristics during puberty. *Int J Hyg Environ Health* 2015;**218**:603–615.
675 Hsieh AC, Ruggero D. Targeting eukaryotic translation initiation factor 4E (eIF4E) in cancer.
676 *Clin Cancer Res* 2010;**16**:4914–4920.

677 Jaiswal D, Trivedi S, Agrawal NK, Singh K. Dysregulation of apoptotic pathway candidate
678 genes and proteins in infertile azoospermia patients. *Fertil Steril* 2015;**104**:736–743.e6.
679 Jansen RS, Addie R, Merkx R, Fish A, Mahakena S, Bleijerveld OB, Altelaar M, IJlst L,
680 Wanders RJ, Borst P, *et al.* N-lactoyl-amino acids are ubiquitous metabolites that originate
681 from CNDP2-mediated reverse proteolysis of lactate and amino acids. *Proc Natl Acad Sci*
682 *U S A* 2015;**112**:6601–6606.
683 Jodar M, Soler-Ventura A, Oliva R. Semen proteomics and male infertility. *J Proteomics*
684 2017;**162**:125–134.
685 Jonsson B. Risk assessment on butylphenol, octylphenol and nonylphenol, and estimated
686 human exposure of alkylphenols from Swedish fish. 2006; Uppsala University Press,
687 Uppsala, Sweden. Available from: http://www.uu.se/digitalAssets/177/c_177024-l_3-
688 k_jonsson-beatrice-report.pdf.
689 Karp NA, Lilley KS. Investigating sample pooling strategies for DIGE experiments to address
690 biological variability. *Proteomics* 2009;**9**:388–397.
691 Kim HJ, Na JI, Min BW, Na JY, Lee KH, Lee JH, Lee YJ, Kim HS, Park JT. Evaluation of
692 protein expression in housekeeping genes across multiple tissues in rats. *Korean J Pathol*
693 2014;**48**:193–200.
694 Klett D, Cahoreau C, Villeret M, Combarnous Y. Effect of pharmaceutical potential endocrine
695 disruptor compounds on protein disulfide isomerase reductase activity using di-eosin-
696 oxidized-glutathion. *PLoS One* 2010;**5**:e9507.
697 Kozlowska E, Krzyzosiak WJ, Koscianska E. Regulation of Huntingtin gene expression by
698 miRNA-137, -214, -148a, and their respective isomiRs. *Int J Mol Sci* 2013;**14**:16999–

17016.

Lambrot R, Muczynski V, Lécureuil C, Angenard G, Coffigny H, Pairault C, Moison D, Frydman R, Habert R, Rouiller-Fabre V. Phthalates impair germ cell development in the human Fetal testis in vitro without change in testosterone production. *Environ Health Perspect* 2009;**117**:32–37.

Langmead B, Trapnell C, Pop M, Salzberg SL. Ultrafast and memory-efficient alignment of short DNA sequences to the human genome. *Genome Biol* 2009;**10**:R25.

Li Z, Zheng Z, Ruan J, Li Z, Zhuang X, Tzeng CM. Integrated analysis miRNA and mRNA profiling in patients with severe oligozoospermia reveals miR-34c-3p downregulates PLCXD3 expression. *Oncotarget* 2016;**7**:52781–52796.

López-Casas PP, Mizrak SC, López-Fernández LA, Paz M, de Rooij DG, del Mazo J. The effects of different endocrine disruptors defining compound-specific alterations of gene expression profiles in the developing testis. *Reprod Toxicol* 2012;**33**:106–115.

Manikkam M, Tracey R, Guerrero-Bosagna C, Skinner MK. Plastics derived endocrine disruptors (BPA, DEHP and DBP) induce epigenetic transgenerational inheritance of obesity, reproductive disease and sperm epimutations. *PLoS One* 2013;**8**:e55387.

Muller H, Marzi MJ, Nicassio F. IsomiRage: from functional classification to differential expression of miRNA isoforms. *Front Bioeng Biotechnol* 2014;**2**:38.

Munoz X, Mata A, Bassas LL, Larriba S. Altered miRNA signature of developing germ-cells in infertile patients relates to the severity of spermatogenic failure and persists in spermatozoa. *Sci Rep* 2015;**5**:17991.

Nagao T, Yoshimura S, Saito Y, Nakagomi M, Usumi K, Ono H. Reproductive effects in male

721 and female rats from neonatal exposure to p-octylphenol. *Reprod Toxicol* 2001;**15**:683–
722 692.
723 National Toxicology Program. NTP-CERHR monograph on the potential human reproductive
724 and developmental effects of di-n-butyl phthalate (DBP). *NTP CERHR MON* 2003a;i-
725 III90. Available from: http://www.ncbi.nlm.nih.gov/pubmed/15995736.
726 National Toxicology Program. NTP-CERHR Monograph on the Potential Human Reproductive
727 and Developmental Effects of Butyl Benzyl Phthalate (BBP). *Ntp Cerhr Mon* 2003b;i-
728 III90. Available from: http://www.ncbi.nlm.nih.gov/pubmed/15995737.
729 National Toxicology Program. NTP-CERHR monograph on the potential human reproductive
730 and developmental effects of di (2-ethylhexyl) phthalate (DEHP). *Natl Institutes Health*
731 2006; NIH Publication No. 06-4476; v, vii-7, II–iii-xiii passim. Available from:
732 http://www.ncbi.nlm.nih.gov/pubmed/19407857.
733 Neilsen CT, Goodall GJ, Bracken CP. IsomiRs - The overlooked repertoire in the dynamic
734 microRNAome. *Trends Genet* 2012;**28**:544–549.
735 Noveski P, Popovska-Jankovic K, Kubelka-Sabit K, Filipovski V, Lazarevski S, Plaseski T,
736 Plaseska-Karanfilska D. MicroRNA expression profiles in testicular biopsies of patients
737 with impaired spermatogenesis. *Andrology* 2016;**4**:1020-1027
738 Pant N, Shukla M, Kumar Patel D, Shukla Y, Mathur N, Kumar Gupta Y, Saxena DK.
739 Correlation of phthalate exposures with semen quality. *Toxicol Appl Pharmacol*
740 2008;**231**:112–116.
741 Patiño-García D, Cruz-Fernandes L, Buñay J, Palomino J, Moreno RD. Reproductive
742 alterations in chronically exposed female mice to environmentally relevant doses of a

743 mixture of phthalates and alkylphenols. *Endocrinology* 2018; **159:1050**-1061.
744 Paz M, Morín M, del Mazo J. Proteome profile changes during mouse testis development.
745 *Comp Biochem Physiol Part D Genomics Proteomics* 2006;**1**:404–415.
746 Primm TP, Gilbert HF. Hormone binding by protein disulfide isomerase, a high capacity
747 hormone reservoir of the endoplasmic reticulum. *J Biol Chem* 2001;**276**:281–286.
748 Radonić A, Thulke S, Mackay IM, Landt O, Siegert W, Nitsche A. Guideline to reference gene
749 selection for quantitative real-time PCR. *Biochem Biophys Res Commun* 2004;**313**:856–
750 862.
751 Rajamani U, Gross AR, Ocampo C, Andres AM, Gottlieb RA, Sareen D. Endocrine disruptors
752 induce perturbations in endoplasmic reticulum and mitochondria of human pluripotent
753 stem cell derivatives. *Nat Commun* 2017;**8**: 219.
754 Rider CV, Furr JR, Wilson VS, Gray LE. Cumulative effects of in utero administration of
755 mixtures of reproductive toxicants that disrupt common target tissues via diverse
756 mechanisms of toxicity. *Int J Androl* 2010;**33**:, p. 443–462.
757 Rogers R, Ouellet G, Brown C, Moyer B, Rasoulpour T, Hixon M. Cross-talk between the Akt
758 and NF-kappaB signaling pathways inhibits MEHP-induced germ cell apoptosis. *Toxicol*
759 *Sci* 2008;**106**:497–508.
760 Siddiqui N, Sonenberg N. Signalling to eIF4E in cancer. *Biochem Soc Trans* 2015;**43**:763–772.
761 Sifakis S, Androutsopoulos VP, Tsatsakis AM, Spandidos DA. Human exposure to endocrine
762 disrupting chemicals: effects on the male and female reproductive systems. *Environ*
763 *Toxicol Pharmacol* 2017;**51**:56–70.
764 Smorag L, Zheng Y, Nolte J, Zechner U, Engel W, Pantakani DV. MicroRNA signature in

765 various cell types of mouse spermatogenesis: evidence for stage-specifically expressed
766 miRNA-221, -203 and -34b-5p mediated spermatogenesis regulation. *Biol Cell*
767 2012;**104**:677–692.
768 Takagi S, Itoh N, Kimura M, Sasao T, Tsukamoto T. Spermatogonial proliferation and
769 apoptosis in hypospermatogenesis associated with nonobstructive azoospermia. *Fertil*
770 *Steril* 2001;**76**:, p. 901–907.
771 Telonis AG, Loher P, Jing Y, Londin E, Rigoutsos I. Beyond the one-locus-one-miRNA
772 paradigm: microRNA isoforms enable deeper insights into breast cancer heterogeneity.
773 *Nucleic Acids Res* 2015;**43**: 9158-75.
774 Tumova J, Andel M, Trnka J. Excess of free fatty acids as a cause of metabolic dysfunction in
775 skeletal muscle. *Physiol Res* 2016; **65:193**-207.
776 Uhlen M, Bandrowski A, Carr S, Edwards A, Ellenberg J, Lundberg E, Rimm DL, Rodriguez
777 H, Hiltke T, Snyder M, *et al.* A proposal for validation of antibodies. *Nat Methods* 2016;
778 **10**:823-7
779 Vera Y, Erkkila K, Wang C, Nunez C, Kyttanen S, Lue Y, Dunkel L, Swerdloff RS, Sinha
780 Hikim AP. Involvement of p38 mitogen-activated protein kinase and inducible nitric oxide
781 synthase in apoptotic signaling of murine and human male germ cells after hormone
782 deprivation. *Mol Endocrinol* 2006;**20**:1597–1609.
783 Vlachos IS, Paraskevopoulou MD, Karagkouni D, Georgakilas G, Vergoulis T, Kanellos I,
784 Anastasopoulos IL, Maniou S, Karathanou K, Kalfakakou D, *et al.* DIANA-TarBase v7.0:
785 Indexing more than half a million experimentally supported miRNA:mRNA interactions.
786 *Nucleic Acids Res* 2015;**43**:D153–D159.

787 Weinkauf M, Hiddemann W, Dreyling M. Sample pooling in 2-D gel electrophoresis: A new
788 approach to reduce nonspecific expression background. *Electrophoresis* 2006;**27**:4555–
789 4558.
790 Wessel D, Flügge UI. A method for the quantitative recovery of protein in dilute solution in the
791 presence of detergents and lipids. *Anal Biochem* 1984;**138**:141–143.
792 Yoshida M, Katsuda SI, Takenaka A, Watanabe G, Taya K, Maekawa A. Effects of neonatal
793 exposure to a high-dose p-tert-octylphenol on the male reproductive tract in rats. *Toxicol*
794 *Lett* 2001;**121**:21–33.
795 Yu Z, Guo R, Ge Y, Ma J, Guan J, Li S, Sun X, Xue S, Han D. Gene expression profiles in
796 different stages of mouse spermatogenic cells during spermatogenesis. *Biol Reprod*
797 2003;**69**:37–47.
798 Zhang Z, Miao L, Xin X, Zhang J, Yang S, Miao M, Kong X, Jiao B. Underexpressed CNDP2
799 participates in gastric cancer growth inhibition through activating the MAPK signaling
800 pathway. *Mol Med* 2014;**20**:17–28.
801 Zhang S, Zhao Y, Lei B, Li C Mao X. PGAM1 is involved in spermatogenic dysfunction and
802 affects cell proliferation, apoptosis, and migration. *Reprod Sci* 2015;**22**:1236–1242.
803 Zhuang X, Li Z, Lin H, Gu L, Lin Q, Lu Z, Tzeng CM. Integrated miRNA and mRNA
804 expression profiling to identify mRNA targets of dysregulated miRNAs in non-obstructive
805 azoospermia. *Sci Rep* 2015;**5**: 7922.
806
807
808 **FIGURE LEGENDS**

Figure 1: Populations of mice exposed to EDCs mixture have compromised fertility.

White diamonds and gray circles indicate male population of control mice (n= 9) and mice exposed to EDCs mixture, (n=12) respectively. Gray circles inside white background indicate populations of mice with a normal potential fertility and without induced pre-implantation losses. Green and red backgrounds indicate the populations of animals in which the parameters were detected as decreased or increased, respectively.

Figure 2: Proteins that changes its expression in mouse testis exposed to EDCs.

A) Up-regulated proteins, B) down-regulated proteins and C) protein showing uniform expression in mouse testis exposed to EDCs compared with control. Each chart represents the relative levels by regression lineal test (LOESS) for PDQuest, significant changes by 1.2-fold. Images are representative picture of 2D-electrophoresis gels in each condition.

Figure 3: Immunolocalisation and up-regulation of PGAM1 in mice testis by the exposure to EDCs mixture

A) PGAM1 protein levels in mice testis exposed to EDCs mixture and/or control were determined by Western blot and normalised with β-ACTIN. All graphics represent the mean ± SEM, n = 4. Unpaired t test, *$p < 0.05$. Abbreviation: AU, arbitrary units. B) Representative pictures of PGAM1 in mouse testes exposed to EDCs mixture and controls, bar = 50 µm.

Figure 4: Cell death is the main molecular function related with dysregulated proteins in testis of mice exposed to EDCs mixture

A) GO enrichment analysis of dysregulated proteins was performed using GlueGO. Enrichment was obtained using hypergeometric distribution test, with a p-value threshold > 0.05. Each colour represents a different metabolic pathway. B) Rate of identified proteins that are involved in cell death. Molecular function was obtained according to the information available at the MGI and UniProt database.

Figure 5: Integrative analyses of dysregulated proteins and miRNAs in mouse testis exposed to EDCs mixture.

A) Hierarchical cluster analysis of differentially expressed miRNAs/isomiRs involved in the post-transcriptional control of dysregulated proteins. Expression levels correspond to log2 normalised read counts using DeSeq tool of the R/Bioconductor software package, in testes of mice exposed to EDCs mixture comparing with control mouse testes. B) Integrative map of interactions between down-regulated miRNAs/isomiRs and overexpressed proteins in mouse testis exposed to EDCs mixture; red colour indicates over-expression and gray to green scale under-expression. C) Prediction of *Eif4E* as target of *miR-15b-5p / miR-3085-3p*_UA_3prime in human and mouse isomiRs nomenclature according to Muller *et al.* (Muller *et al.*, 2014).

Figure 6: Common proteins and miRNAs differentially expressed by the exposure of EDCs on mouse testis and in idiopathic infertile human males.

A) Comparative analyses of dysregulated proteins in humans with spermatogenic failure (Alikhani *et al.*, 2017) and in mouse testis exposed to EDCs. B) Comparative analyses of dysregulated microRNAs in humans with spermatogenic failure (Abu-Halima *et al.*, 2014;

Munoz *et al.*, 2015; Noveski *et al.*, 2016) and in mouse testis exposed to EDCs (Buñay *et al.*, 2017). The name in parenthesis refers to the reference of the study.

SUPPLEMENTARY FIGURE LEGENDS

Supplementary Figure 1: 2D-Protein profiles changes in mouse testis exposed to EDCs mixture.

A) 180 μg of soluble protein extracts from testes of adult mice from the control group and the group exposed to EDCs mixture were subjected to 2D electrophoresis. Gels were stained with SYPRO-Ruby. Circled spots with their corresponding identification number were selected by PDQuest software and analyzed by MALDI-TOF. B) Local regression scatter plot of proteins/spots quantities (intensity of protein spots). The quantity of each protein/spot of control samples (X-axis) is plotted on a logarithmic scale against the quantity of each protein/spot of exposed to EDCs mixture samples (Y-axis). Blue and red lines show 2-fold up-regulated and down-regulated proteins/spots respectively. The linear regression can be seen in green.

Supplementary Figure 2: Relative fold changes of proteins identified after the normalisation by endogenous reference protein (PPIA).

Supplementary Figure 3: Predicted protein-protein interaction networks of dysregulated proteins due to the exposure to EDCs mixture.

Nodes represent proteins and edges represent the predicted functional associations inferred by STRING database.

Table I: Changes in the proteome of mice testis exposed to EDCs mixture.

Spot No. [1]	Ac. Code. [2]	Symbol	Protein Name	MM (Da) /pI theor [3-4].	Mat'db peps[5].	Total Score [6]	Sequence coverage (%) [7]	Molecular function [8]	Biological process [8]
A. Proteins up-regulated by the exposure to EDCs mixture and involved in germ cell death									

203	Q9JIQ3	DIABLO	Diablo homolog, mitochondrial	26975 / 6.3	7	305	32	Activating caspases. Inhibitory activity (IAP)	Intrinsic apoptotic signaling pathway
5101	P70349	HINT1	Histidine triad nucleotide-binding protein 1	13882 /6.36	5	157	58	Hydrolase activity	Intrinsic apoptotic signaling pathway by p53 class mediator, positive regulation of calcium-mediated signaling
4301	P63073	EIF4E	Eukaryotic translation initiation factor 4E	25266 / 5.79	4	236	18	Eukaryotic initiation factor 4G binding,	Regulation of translation, positive regulation of mitotic cell cycle, behavioural fear response
3202	P99026	PSMB4	Proteasome subunit beta type-4	29211 / 5.47	7	162	37	Threonine-type endopeptidase activity	Proteasome-mediated ubiquitin-dependent protein catabolic process
3702	Q9D1A2	CNDP2	Cytosolic nonspecific dipeptidase	53190 /5.43	6	131	12	Dipeptidase activity	Proteolysis
7101	Q01768	NME2	Nucleoside diphosphate kinase B	17466 / 6.97	9	505	51	Nucleoside diphosphate kinase activity, fatty acid binding	Mitophagy in response to mitochondrial depolarization, cellular response to fatty acid, glucose stimulus and oxidative stress
6401	Q9DBJ1	PGAM1	Phosphoglycerate mutase 1	28928 / 6.67	7	365	40	Phosphoglycerate mutase activity, protein kinase binding	Glycolytic process
5605	Q9JHI5	IVD	Isovaleryl-CoA dehydrogenase, mitochondrial	46695 / 8.53	5	200	12	Isovaleryl-CoA dehydrogenase activity, fatty-acyl-CoA binding	Lipid homeostasis
B. Proteins down-regulated by the exposure to EDCs mixture and involved in germ cell death									
0	Q8CHP8	PGP	phosphoglycolate phosphatase	34975 / 5.21	6	170	42	Magnesium ion binding, phosphoglycolate phosphatase activity,	Carbohydrate metabolic process, dephosphorylation, peptidyl-tyrosine dephosphorylation
2901	P63017	HSPA8	Heat shock cognate 71 kDa protein	71055 / 5.37	8	362	18	ATPase activity, poly(A) RNA binding, unfolded protein binding	ATP metabolic process, chaperone mediated protein folding requiring cofactor,
3804	P30416	FKBP4	Peptidyl-prolyl cis-trans isomerase FKBP4	51939 / 5.54	14	367	38	ATP binding, glucocorticoid receptor binding, poly(A) RNA binding	Androgen receptor signaling pathway, embryo implantation, male sex differentiation, reproductive structure development

3807	P27773	PDIA3	Protein disulfide-isomerase A3	57099 / 5.88	14	400	30	Poly(A) RNA binding, protein disulfide isomerase activity	Cell redox homeostasis, positive regulation of extrinsic apoptotic signaling pathway, protein folding
6302	P15626	GSTM2	Glutathione S-transferase Mu 2	25871 /6.9	12	455	65	Glutathione transferase activity	Glutathione metabolic process, xenobiotic catabolic process
5308	Q80W21	GSTM7	Glutathione S-transferase Mu 7	25864 / 6.34	4	71	20	Glutathione transferase activity, receptor binding	Glutathione metabolic process, regulation of release of sequestered calcium ion into cytosol by sarcoplasmic reticulum, xenobiotic catabolic process
5705	P80314	CCT2	T-complex protein 1 subunit beta	57783 / 5.97	12	541	28	ATP binding, ubiquitin protein ligase binding	Binding of sperm to zona pellucida, chaperone-mediated protein complex assembly, toxin transport
7401	Q60930	VDAC2	Voltage-dependent anion-selective channel protein 2	32340 / 7.44	6	180	31	Voltage-gated anion channel activity, nucleotide binding	Negative regulation of intrinsic apoptotic signaling pathway, negative regulation of protein polymerization
C. Other up-regulated proteins identified									
3601	Q924M7	MPI	Mannose-6-phosphate isomerase	47229 / 5.62	7	211	23	Mannose-6-phosphate isomerase activity,	Mannose to fructose-6-phosphate metabolic process
6303	Q9CQE8	RTRAF	RNA transcription, translation and transport factor protein	28249 / 6.4	5	215	26	Poly(A) RNA binding, identical protein binding	Positive regulation of transcription from RNA polymerase II promoter, tRNA splicing, negative regulation of protein kinase activity
D. Other proteins identified									
8102	P17742	Ppia	Peptidyl-prolyl cis-trans isomerase A	18131 / 7.74	6	320	53	Poly(A) RNA binding, peptide binding	Positive regulation of protein secretion, lipid particle organization, protein folding

Data depicted correspond to the most statistically significant candidates encoded in *Mus musculus*.

[1] Spot numbering as shown in the 2D-gels depicted in Supplementary Figure 1

[2] Protein accession code from *Mus musculus* database

[3] Theoretical molecular weight (Da) - [4]Theoretical isoelectric point (pI)
[5] Number of matched peptides
[6] Mascot Total score is -10*Log(P), where P is the probability that the observed match is a random event
[7] Sequence coverage is the amino acids ratio (no. identified in peptides/no. in theoretical peptides from sequence data) expressed as a percentage
[8] Ontology classification according Mouse Genome Informatics (M.G.I.) and UniprotKB

894

895

896

897
898

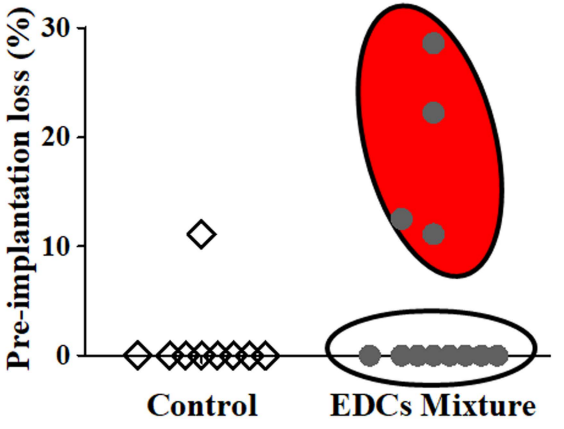

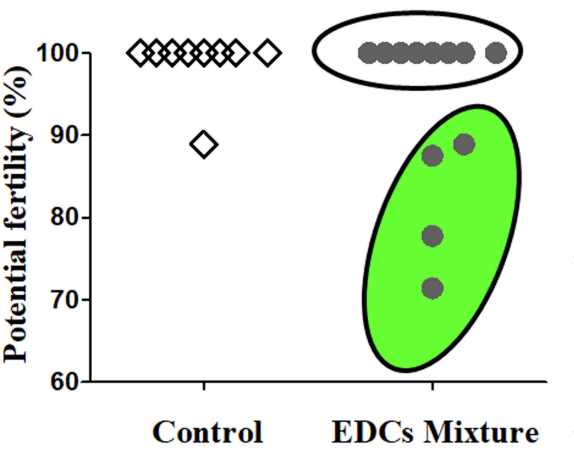

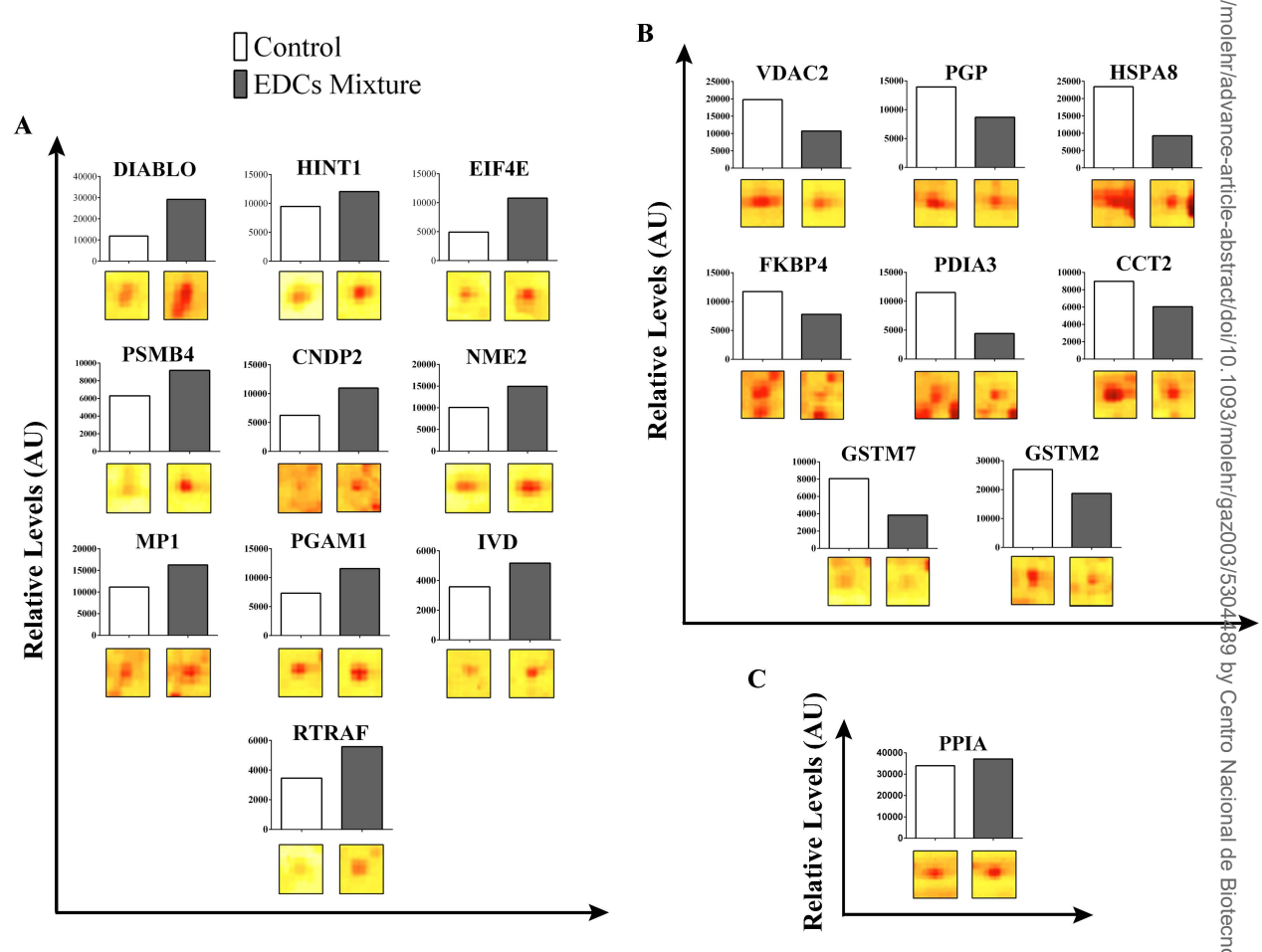

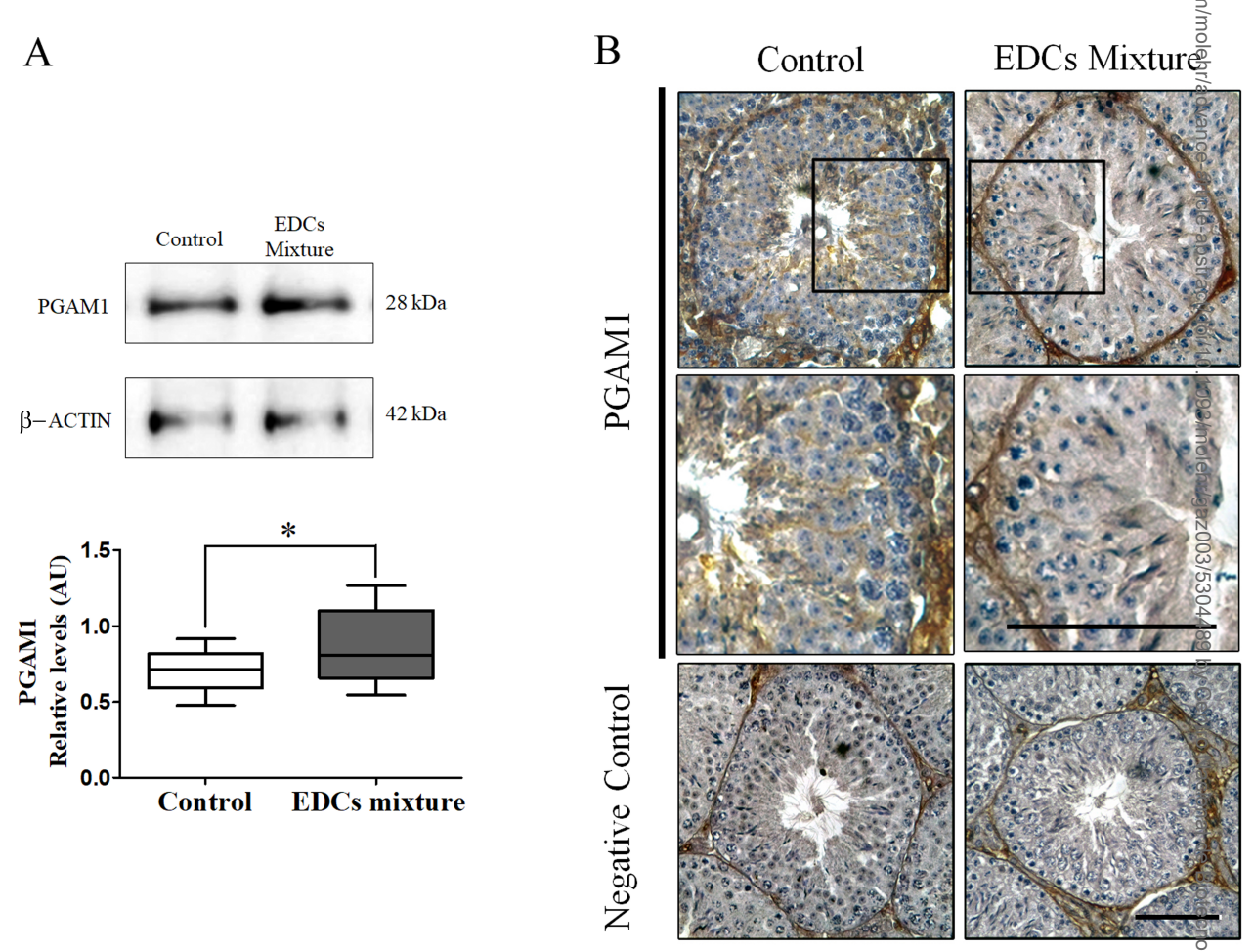
A
Control
EDCs Mixture
PGAM1
28 kDa
β–ACTIN
42 kDa
*
PGAM1 Relative levels (AU)
1.5
1.0
0.5
0.0
Control
EDCs mixture
B
Control
EDCs Mixture
PGAM1
Negative Control